Influence Of Stream-Groundwater Interactions In The Streambed Sediments On NO3 Flux To A Low-Relief Coastal Stream

Gu, Chuanhui * Hornberger, G.M. * Herman, J.S. * Mills, A. L. *

Water-saturated, organic-rich sediments immediately surrounding a stream channel can provide a protective buffer between streams and adjacent land-based activities by removing plant nutrients from shallow groundwater flowing through them, but the hydrological factors that influence the effectiveness of nitrate removal are not well characterized. A two-dimensional, fully distributed, variably saturated flow and transport model was evaluated for its success in using mechanisms of biological reaction in streambed sediments to quantify nitrate flux into the stream under base flow conditions. The model was used to interpret the observed hydrological dynamics during storms at Cobb Mill Creek, Virginia. During base flow conditions, relatively deep groundwater flow paths carrying water containing high nitrate concentrations discharged through the streambed sediments, and high denitrification rates were observed along with a substantial reduction in the nitrate concentration. During storm events, reduced discharge of groundwater in the face of a diminished hydraulic gradient during passage of a flood wave led to longer residence times for water in the biologically active sediments underlying the stream channel, thus providing an opportunity for enhanced denitrification to further reduce nitrate loads to the stream. We conclude that in cases of low-relief streams with substantial hillslopes adjacent to the stream combined with transmissive sediments, storm events can actually contribute to enhanced removal of nitrate locally (at the hillslope scale) as opposed to a simple lowering of concentration due to dilution.

Gu, Chuanhui, Mills, A.L., Hornberger, G.M. **(2008).** "Influence of stream-groundwater interactions in the streambed sediments on NO3- flux to a low-relief coastal stream," Original version available in: Water Resources Research.. 44, W11432, [**DOI**:10.1029/2007WR006739], [**ISSN**: 0097-8078].

Influence of stream-groundwater interactions in the streambed sediments on NO3 flux to a low-relief coastal stream

1. Introduction

[2] Nitrate transport to streams has received considerable attention because of enhanced eutrophication of receiving waters. Denitrification, the biological conversion of NO_3^- to N_2, is of importance in riparian zones and particularly in streambed sediments [*Gu et al.*, 2007; *Hedin et al.*, 1998; *Hill*, 1996; *Hill et al.*, 2000]. The extent to which biogeochemical processes influence contaminant transport depends on the relative rates of water transport and biological reactions [*Brusseau et al.*, 1999; *Gu et al.*, 2007; *Ocampo et al.*, 2006]. Groundwater discharges during base flow and storms can have different residence times that can influence the extent of biological reactions [*Gu et al.*, 2007]. In addition, flow paths are affected strongly by topography, and in some cases, discharging groundwater can bypass zones of high organic carbon content that are the sites of biogeochemical reactions. For example, *Puckett and Hughes* [2005] found limited NO_3^- removal within a riparian aquifer adjacent to a coastal stream. They proposed that the coarser-grained sediments in the surficial aquifer provided a preferential flow path that allowed NO_3^- in groundwater to pass beneath the shallow reducing layer in the riparian zone and to discharge directly into the streambed. *Inamdar and Mitchell* [2006] found that steep hillslopes can lead to low removal of biologically active constituents in some riparian wetlands.

[3] We have measured high rates of denitrification in streambed sediment cores taken from a field site in coastal Virginia [*Gu et al.*, 2007], but the site is one with a relatively steep hillslope leading to the stream. An unanswered question is whether rates of NO_3^- removal observed in the field situation will reflect the (high) laboratory rates obtained in one-dimensional cores or whether multidimensional flow paths in the field will lead to significant bypassing of the biologically active zones.

[4] During storms, head gradients in streambed sediments of gaining streams can be lessened or reversed as stream stage rises. The transport of nitrate to streams is made more complex as a result. In agricultural catchments, nitrate in streams may show a ''dilution response'' during a storm event under conditions when groundwater is a dominant source of water to the stream but also can show a ''concentration response'' when relatively high nitrate ground-

water is flushed into the stream during events [*Böhlke et al.*, 2007; *Poor and McDonnell*, 2007]. Denitrification in streambed sediments will be affected by flow transients and thus may influence dilution or concentration responses. Laboratory and modeling results indicate that denitrification can remain an important process across storm events in channels [*Gu et al.*, 2008], but how these results extend to the field is unknown. At our field site on the coastal plain of Virginia, the primary nitrate removal mechanism is dentrification in streambed sediments. Because residence time of upwelling groundwater within the streambed sediments controls the extent of nitrate removal [*Gu et al.*, 2007, 2008], temporal changes in hydraulic gradients in the sediments during a storm may result in temporally varying nitrate fluxes to the stream because of both changing flows through the sediments and changing concentrations within those waters. The extent to which temporally varying groundwater residence times in streambed sediments impact dilution or concentration responses in stream nitrate concentrations is unknown.

[5] In this paper, we consider three questions. (1) Do the high rates of denitrification that we measure in laboratory cores adequately reflect mechanisms at the field scale; that is, does consideration of flow paths in two dimensions preserve the inferences about the importance of denitrification in streambed sediments under steady base flow conditions [*Gu et al.*, 2007]? (2) How do groundwater heads in the riparian zone vary across storm events, and can they be successfully described using a two-dimensional groundwater flow model? (3) If a satisfactory model for groundwater heads can be formulated, can it be used to drive a reactive transport model to explain both the steady state (base flow) nitrate flux to the stream and the changes in the flux over storm events?

[6] We report a combined modeling and field monitoring study of hydrological interactions within a hillslope to examine the hydrological control on NO_3^- transport and loading to the adjacent stream. Measurements were made at Cobb Mill Creek, Virginia, which drains a small catchment on the coastal plain of Virginia. Hydrological fluxes during base flow and during several small flood events were determined. The field measurements were interpreted using a two-dimensional, finite element model of a cross section through the hillslope and channel. The results of this study indicate that our field observations are consistent with inferences about the importance of residence time of groundwater in streambed sediments drawn from experiments on laboratory cores reported by *Gu et al.* [2007]. Field observations interpreted with flow and transport models confirm that nitrate reduction in the streambed sediments is the major removal mechanism of nitrate at our site. Furthermore, we infer that the NO_3^- dilution pattern observed during storms was caused, at least partially, by a reduced streamward gradient of groundwater that leads to longer residence time of discharging water within biologically active sediments near the groundwater-surface water interface, providing an extended opportunity for denitrification to remove NO_3^- from the discharging groundwater.

2. Field Site

[7] Cobb Mill Creek drains a 4.96 km^2 low-relief coastal plain catchment, located 19 miles north of the mouth of the Chesapeake Bay on the Eastern Shore of Virginia at the Anheuser-Busch Coastal Research Center (Figure 1). Land use in the catchment is dominated by forested (62%) and agricultural (34%) areas, with the remaining 4% of land area in residential, commercial, highway, and other uses. Groundwater discharging to Cobb Mill Creek comes from the unconfined Columbia aquifer, composed of Pleistocene-aged unconsolidated sands (generally 8–30 m thick [*Sinnott and Tibbits*, 1968; *Mixon et al.*, 1989], in accord with measurements made at a location near our field site [*Hubbard et al.*, 2001]) with high hydraulic conductivity $\sim 5 \times 10^{-5}$ m s^{-1} obtained by rising head slug tests in the field immediately upslope of the experimental site. These values agree well with those obtained by *Hubbard et al.* [2001] ($5.53 \times 10^{-5} \pm 1.56 \times 10^{-8}$ m s^{-1}) at a site about 1.6 km away in the same formation. The Upper Yorktown confining layer forms the base of the Columbia aquifer.

[8] Cobb Mill Creek is a first-order tidal creek that drains into Oyster Harbor. It is a groundwater-dominated stream surrounded by a riparian forest. Surface relief is generally low, with greater slopes along regions immediately adjacent to the streams. The majority of the length of Cobb Mill Creek is freshwater and nontidal. A hillslope upstream from the tidal zone was chosen as the focus of our observational work (Figures 1 and 2). A sand-bottom channel with a water depth of 20–40 cm characterizes this part of the reach.

3. Methods

3.1. Field Methods

[9] A network of 16 wells and 10 piezometer nests was installed on the hillslope to monitor the spatial and temporal patterns of nitrate concentrations and hydrological conditions in the subsurface (Figure 1). Wells and piezometers were constructed of 2.54-cm PVC well casing. Wells penetrate 1.5 to 5 m below the water table and are screened at least 1 m above the maximum water table. A single transect of six shallow, partially penetrating wells and piezometer nests, S1, N1, N3, N7, N9, and N11, crossed the hillslope, nearly perpendicular to the stream and parallel to the direction of the shallow groundwater flow (Figure 2). This hillslope transect is characterized by a relatively steep slope immediately adjacent to the incised stream channel, which is about 1.2 m deep. The entire hillslope site was surveyed with mean sea level as the datum to establish the elevation of the monitoring wells (and thus the elevation of the hydraulic head) and the topography of the site. Groundwater elevation and stream stage were measured simultaneously at 10-min intervals with pressure transducers (Solinst, Inc., Georgetown, Ontario, Canada) installed in well N1 and a stilling well in the stream. Measurements obtained from August to December 2005 were used to investigate the transient hydrological response of the hillslope. The sandy soils at the site are very permeable; we have not observed overland flow or any evidence of overland flow at this site for events of modest size such as we investigate here. Storm event sampling occurred during the fall of 2006. Similar weather conditions occurred during the fall of 2005 and 2006, so we deem that the transient stream chemistry study of 2006 based on the understanding of hillslope hydrology in the previous year was justified.

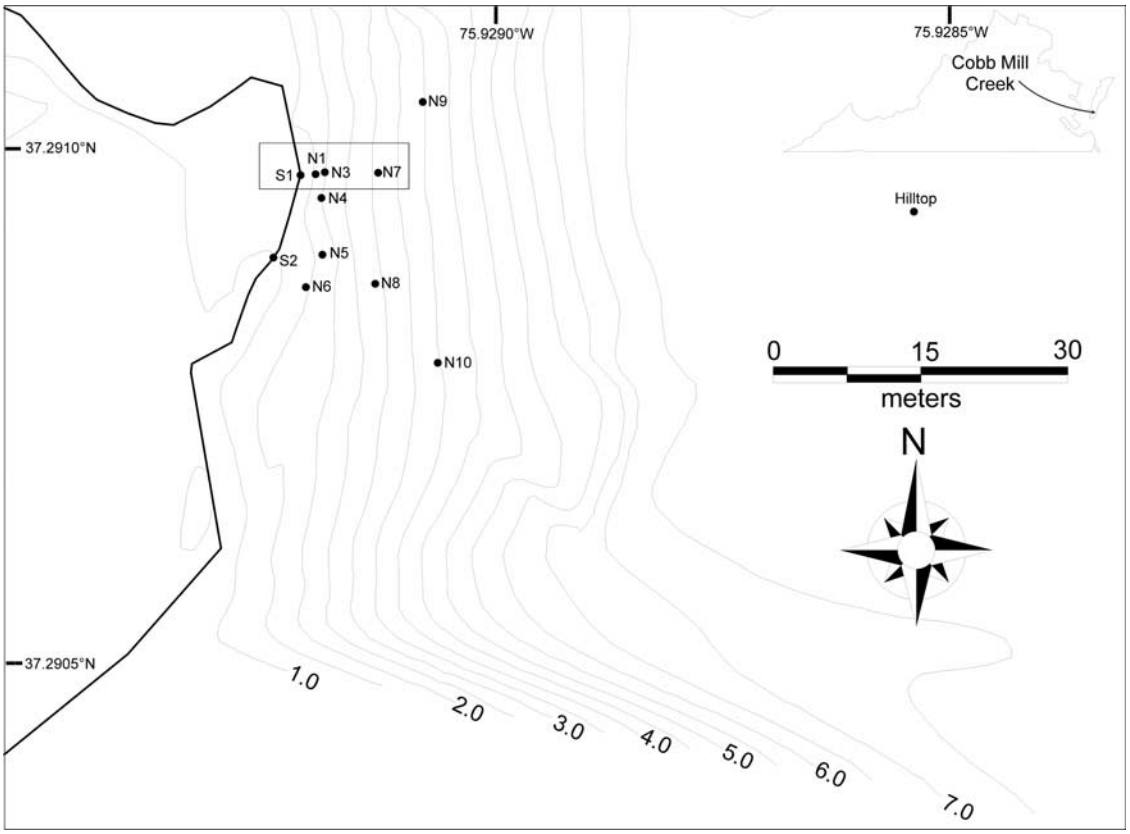

Figure 1. Plan view of the experimental hillslope at Cobb Mill Creek showing the study transect, piezometer locations and contours (1.0-m intervals) of the surface topography. Piezometers numbered with an N are on the hillslope, and those numbered with an S are in the stream itself. The stream flows from north to south in the study reach.

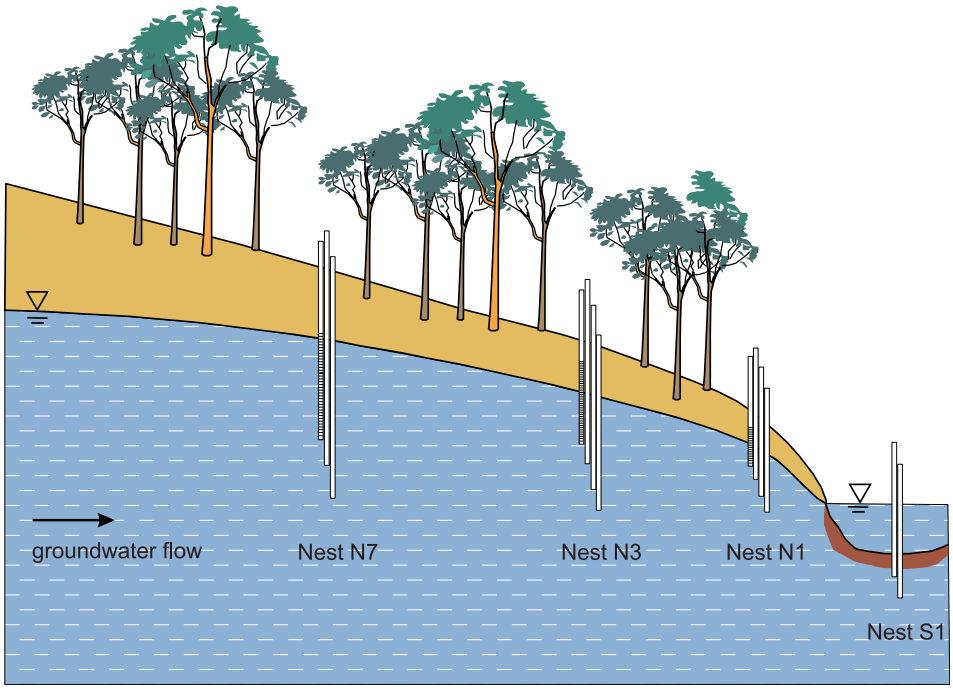

Figure 2. Schematic cross section of the experimental transect at the Cobb Mill Creek site. Each piezometer nest consists of a well and several piezometers with openings at different depths (not all piezometer nests along the transect are shown). The dark area bordering the stream channel represents highly biologically active streambed sediments.

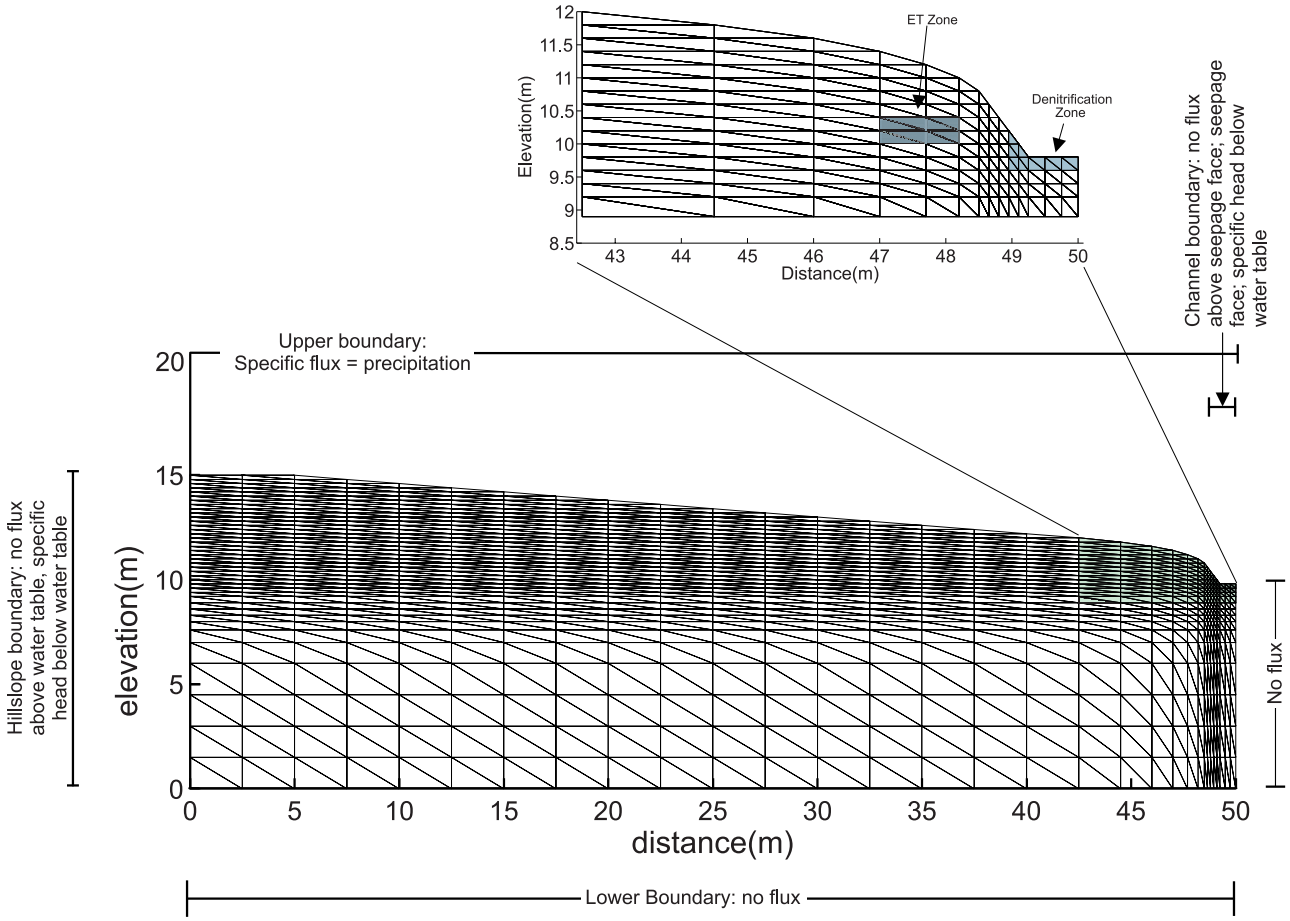

Figure 3. Finite element meshes and boundary conditions constructed for the Cobb Mill Creek transect. The mesh consists of 1068 nodes and 2004 linear, triangular finite elements. The shaded subdomain near the stream was used for the transport model, and the inset shows where evapotranspiration and reaction terms were applied.

[10] Storm event sampling conducted as part of a senior thesis project [*Sofranko*, 2007] for storms during 27–30 October and 8–11 November 2006 was accomplished using a stage-activated interval sampler (Teledyne Isco, Inc., Lincoln, Nebraska). The automated sampler was triggered for event sampling when the stream stage rose above a threshold of 5 cm. The sampler was programmed to sample at 1-h intervals. All samples were collected within 24 h of an event in 500-mL plastic bottles. Concentrations of NO_3^- and Cl^- were measured by ion chromatography.

3.2. Model Development

[11] The aim of the modeling effort was to examine whether denitrification rates observed in cores of streambed sediments at the site [*Gu et al.*, 2007] would describe field conditions when coupled with a reasonable model for groundwater flow. That is, we investigate whether calculated values of flow-weighted nitrate concentrations in the stream are in reasonable agreement with concentrations observed in the stream during base flow and during storm events. The available data are relatively sparse, so absolute accuracy of a calibrated model was not the goal. Rather, our aim is to examine the plausibility of the idea that the observed difference between concentrations of nitrate in stream water ($\sim$2 mg NO_3^--N L^{-1}) and concentrations in groundwater ($\sim$15 mg NO_3^--N L^{-1}) under base flow conditions can be ascribed to denitrification in streambed sediments. We also examine if changes in groundwater residence times within streambed sediments over the relatively short time scales of rainfall events can significantly affect nitrate flux to streams such as Cobb Mill Creek.

[12] A two-dimensional (vertical slice) numerical model was developed to simulate the effects of stream-groundwater interactions on the fate and transport of nitrate in the subsurface adjacent to and underlying the stream (Figures 2 and 3). The numerical model comprised a saturated-unsaturated flow module and a contaminant fate and transport module (see Appendix A for details).

[13] The flow model was applied on a vertical cross section 16 m by 50 m through the riparian zone (Figure 3). The model domain in the region of the stream represents half the channel width, with the vertical boundary at the center of the stream channel specified as a no-flow boundary. The aquifer is about 10 m thick [*Hubbard et al.*, 2001; *Mixon*, 1985]; a no-flow boundary is assumed at the base of the domain. Hydraulic head recorded at a hilltop well showed that the upland water table is fairly stable during transient rainfall events. Thus, the hilltop hydraulic head was set at a constant head of 3.0 m above stream level at base flow. The stream stage was used to specify the

Table 1. Soil Parameters Selected for the Hillslope-Stream Model

Soil Hydraulic Parameter	Value
Brooks-Corey empirical parameter a	10
Brooks-Corey empirical parameter c	4
Brooks-Corey empirical parameter d	2
Residual water saturation S_r	0.1
Specific storage S_s	1×10^{-4}
Horizontal aquifer saturated hydraulic conductivity K (m d^{-1})	2
Horizontal channel saturated hydraulic conductivity K (m d^{-1})	1
Anisotropy ratio	0.2
Porosity θ	0.3
Recharge rate (m d^{-1})	1×10^{-3}

boundary condition on the right-hand side of the mesh. A seepage face was allowed to develop during the falling limb of the hydrograph along the creek bank. Seepage face nodes were assigned a pressure equal to atmospheric pressure (zero). All boundary nodes on the creek bank above the stage and seepage face were assigned no-flow boundary conditions. A constant recharge rate of 10^{-3} m d^{-1} was applied uniformly at the top of the domain. Extrapolated over the entire catchment with the assumption that all recharge enters the stream, this recharge rate would translate to a steady stream discharge of 0.06 m^3 s^{-1}, a value consistent with base flow discharge measurements at our site. The flow model was calibrated by adjusting the saturated hydraulic conductivity to match observed heads in the piezometers during base flow conditions, assuming a homogeneous medium. All other model parameters were estimated on the basis of general information for sandy soils (see Appendix A for details).

[14] Simulations for rainfall events used the calibrated values for hydraulic conductivity for base flow conditions. The initial pressure heads at each computational node for each flow simulation were established using a steady state solution with time-constant boundary conditions representing piezometric heads at the start of each event. The upper boundary was prescribed by setting a flux equal to the measured rainfall rates for that event.

[15] Rainfall infiltrating the agricultural field at the top of the slope is the source of nitrate recharged to groundwater. Rainfall infiltrating along the forested slope, particularly near the stream itself, leads to lower nitrate concentrations at shallow depths than those observed at greater depth and in the hilltop well [*Galavotti*, 2004; *Gu*, 2007; *Mills et al.*, 2008]. Further, our measurements of nitrate concentrations in wells and piezometers indicate that the near-stream sediments are the main area of biological reduction of NO_3^- [*Galavotti*, 2004; *Mills et al.*, 2008]. In aggregate, mixing of water with different NO_3^- signatures occurs in the near-stream area. On the basis of these observations, the reactive transport model was applied to a subdomain (the shaded area in Figure 3). It represents a vertical cross section of 8 m by 2 m near the stream. The transport model consists of an advection term with velocities taken directly from the flow model as described, a dispersion term calibrated on the basis of an assumed conservative tracer (see below), and a reaction term based on local measurements of nitrate reduction.

[16] Observed concentrations of chloride, Cl^-, were used to calibrate the dispersion terms in the transport model. Boundary conditions were specified as zero concentration gradient at each side of the model domain except for the left-hand boundary and the bottom boundary. A constant Cl^- concentration of 16 mg L^{-1} was assigned at the left and bottom sides of the model domain on the basis of measurements from the wells and piezometers. Chloride concentrations in shallow groundwater near the stream were observed to be well above those measured in deeper groundwater [*Galavotti*, 2004; *Gu*, 2007; *Mills et al.*, 2008]. *Hill et al.* [2000] also found high groundwater Cl^- concentration of 40–75 mg L^{-1} in a forested riparian zone in southern Ontario, Canada. This pattern presumably reflects activity of riparian vegetation. A Cl^- source zone was applied in the stream bank area (Figure 3). The location of this source zone and the production rate of Cl^- within it were adjusted along with the dispersion values to calibrate the model.

[17] After calibration, the transport model was applied to simulate NO_3^- distribution along the transect by adding a reaction term to account for nitrate reduction. In this study, we used a multiple-Monod equation to describe microbial reactions, with both organic carbon and dissolved oxygen potentially limiting the reaction (see *Gu et al.* [2007] for details). Boundary conditions were specified as zero concentration gradient at each side of the model domain except for the left-hand boundary and the bottom boundary. The left-hand boundary was assigned a NO_3^- concentration grading from 6 mg NO_3^--N L^{-1} at the surface to 15 mg NO_3^--N L^{-1} at the base. This distribution was chosen as representative of field measurements at our site. The bottom boundary condition was set at 15 mg NO_3^--N L^{-1}, again to represent field observations. A reaction term in the model was specified near the stream channel (Figure 3) to simulate denitrification (see Appendix A for details). The model structure (Monod kinetics) and parameter values (Table 1) derived from laboratory experiments on cores of streambed sediments from our site were used in the model [*Gu*, 2007; *Gu et al.*, 2007].

4. Results

4.1. Steady Flow

[18] For the calibrated flow model (Figure 4), the maximum difference of simulated and observed groundwater heads was 0.12 m. The residuals were unbiased with a mean of 0, indicating that the model simulates heads reasonably, although the model slightly overpredicted the observed near-stream hydraulic heads and underpredicted observed upslope hydraulic heads. The simulated groundwater seepage rate through the stream sediment is about 0.2 m d^{-1}. This value agrees well with the field-determined upward seepage values of 0.12–0.31 m d^{-1} [*Gu*, 2007].

[19] Simulations show that groundwater flows through the hillslope basically horizontally until it approaches the near-stream zone, where the flow direction gradually begins to bend upward (Figure 4). The calculated flow paths through the near-stream segment are used for the transport model.

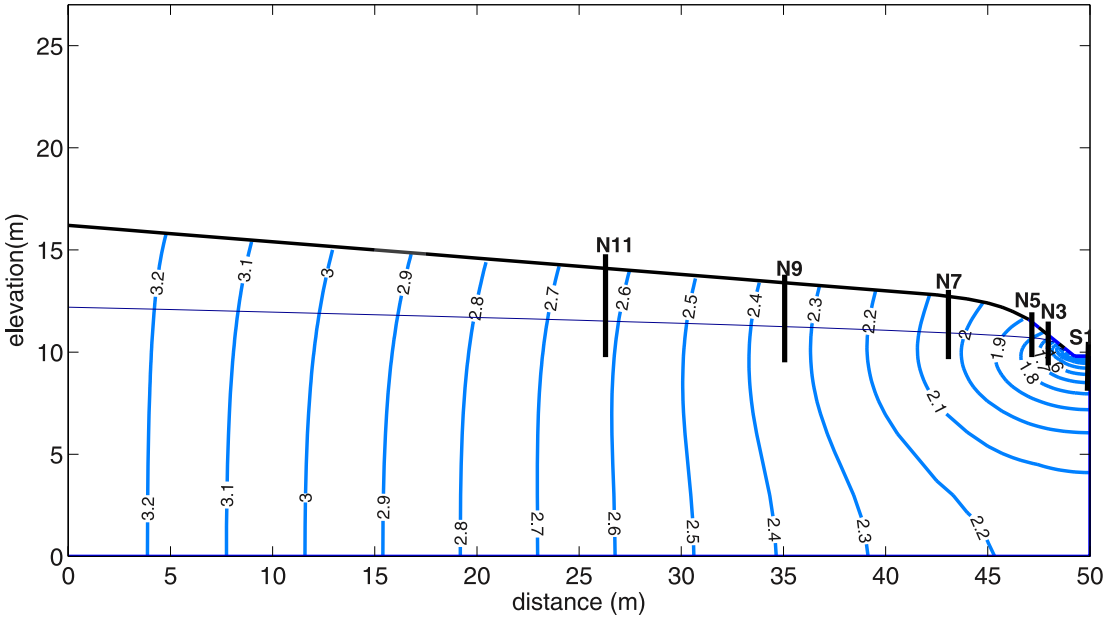

Figure 4. Model-simulated prestorm steady state hydraulic head distribution. Locations of the piezometers internal to the domain are also shown. Elevations are in meters above the base of the flow domain.

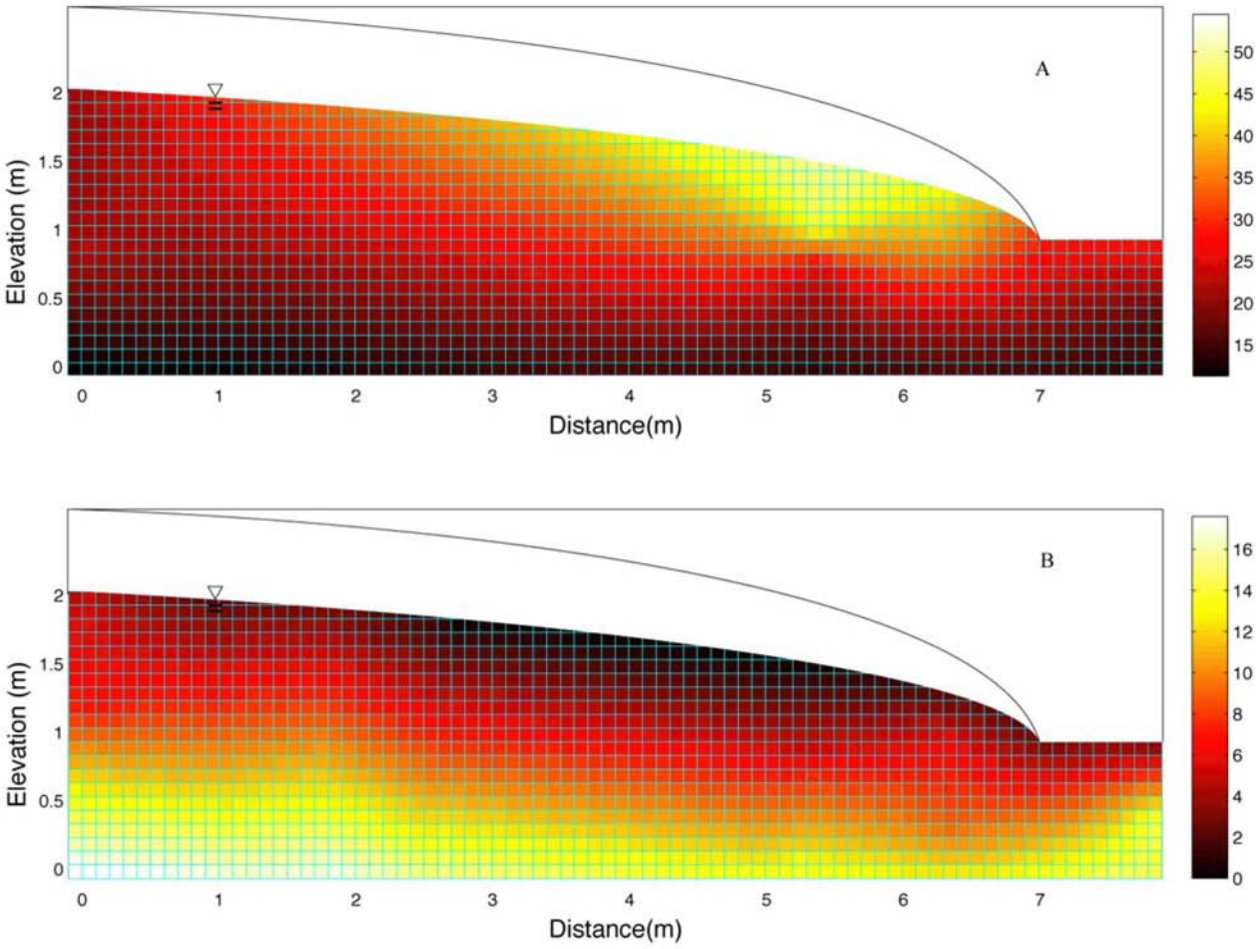

Figure 5. Cross-section view of observed interpolated mean (a) chloride, in mg L^{-1}, and (b) nitrate, in mg NO_3^--N L^{-1}, concentrations. Elevations shown are in meters above the base of the transport model domain.

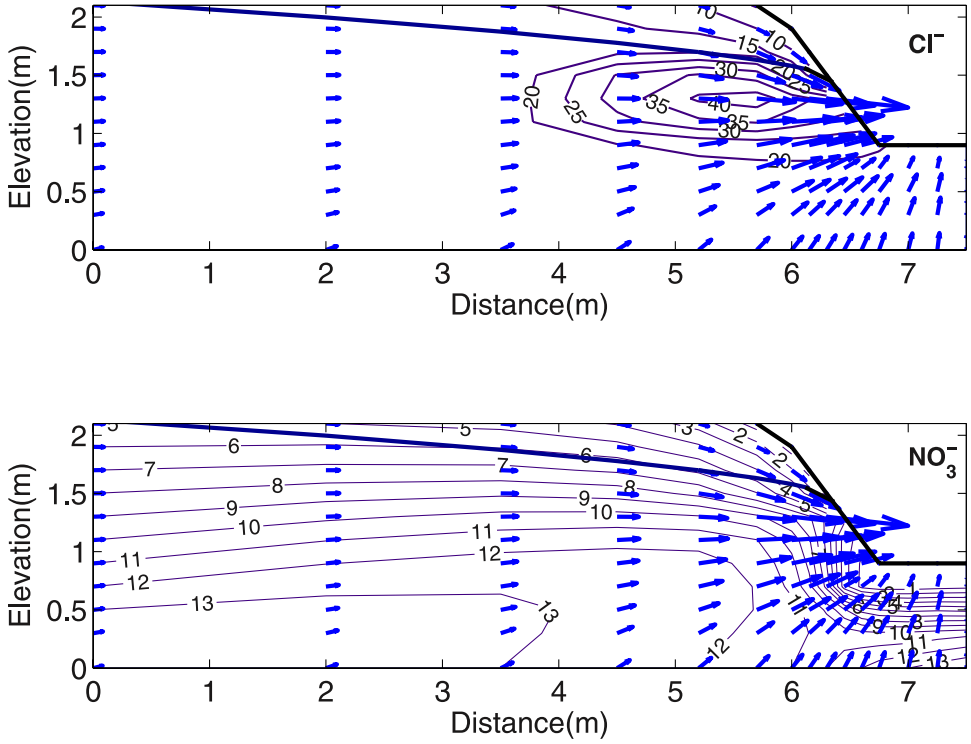

Figure 6. Simulated groundwater flow and Cl^- and NO_3^- concentration in the experimental section. Contours are plotted for units of mg L^{-1} of Cl^- and NO_3^--N, respectively. Elevations shown are in meters above the base of the transport model domain.

4.2. Chloride and Nitrate Concentrations in the Hillslope Riparian Zone

[20] Concentrations of chloride in the stream vary temporally under base flow conditions, but no pattern, including seasonal variation, is evident in our history of observations at the site that includes intermittent sampling that covers all seasons over a 7-year period, 2001 to present. For example, nitrate concentrations in the stream vary from ~1.5 mg NO_3^--N L^{-1} to ~3 mg NO_3^--N L^{-1} but without evident pattern and a mean value close to 2.5 mg NO_3−N L^{-1}. We took long-term average concentrations to represent base flow conditions.

[21] The 3-year mean nitrate and chloride concentrations in groundwater were about 20 mg L^{-1} and about 45 mg L^{-1}, respectively, in the area next to the stream where the water table is close to the surface (Figure 5). Nitrate concentrations showed a distinct trend from relatively low (~2 mg NO_3^--N L^{-1}) near the water table to relatively high (~15 mg NO_3^--N L^{-1}) at depth. This pattern reflects the source of nitrate to deeper groundwater from the area at the top of the hillslope that has been cultivated, with significant fertilizer applied. The stream riparian area is forested and not fertilized, however, so the local recharge in this area leads to much lower concentrations of nitrate near the water table.

4.3. Steady State Cl^- and NO_3^- Distributions

[22] After calibration by adjusting the area where evapoconcentration occurs, the numerical model successfully reproduced the Cl^- concentrations (Figure 6). The simulated concentration distributions of NO_3^-, taking into account denitrification in the near-stream region (the model elements around the stream channel), reproduces the general patterns observed (Figure 6).

[23] When the transport model was run without denitrification, pure mixing of shallow and deep groundwater produced a flow-weighted NO_3^- concentration of 11.3 mg NO_3^--N L^{-1} outflow from the hillslope (compared with measured concentrations of 2.5 mg NO_3^--N L^{-1} in the stream), and the simulated spatial pattern of NO_3^- in the hillslope failed to mimic the observed pattern. The inclusion of the denitrification reaction within the streambed sediments, on the other hand, produced a flow-weighted concentration of 2.44 mg NO_3^--N L^{-1} to the stream and a pattern that was consistent with that observed (cf. Figures 5 and 6). The model produced a sharp NO_3^- concentration gradient in the sediments immediately surrounding the stream channel (Figure 6) similar to that observed in cores [*Gu et al.*, 2008].

4.4. Response of Piezometric Heads to Storms

[24] Measurements of precipitation and of water levels were made during August–December 2005 (Figure 7). A frequency domain low-pass filter [*Hornberger and Wiberg*, 2005] was applied to the transducer data to remove frequencies higher than the diurnal signals. During the period of 20 August 2005 to 20 December 2005, the water table in N1 changed approximately in parallel with the stream stage (Figure 7). Three small storm events during the observation period, labeled from A to C in chronological sequence (Figure 7), were chosen for analysis. The maximum stream stage rise in each of the three events was no more than 30 cm, indicating that overbank flow did not occur. Stream stage showed a prompt rise in response to rainfall events,

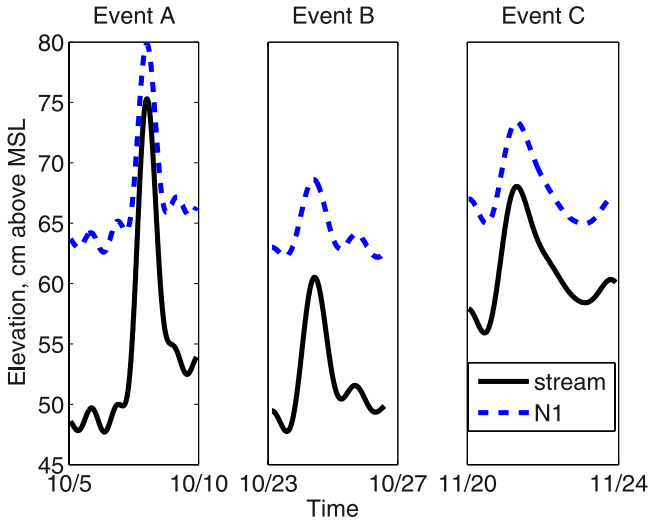

Figure 7. Time series of hydrometric measurements during the period of 20 August to 20 December 2005. Stream stage and hydraulic heads in N1 (note that the data were filtered to remove higher-than-daily frequencies). Three events were selected to study transient processes.

accompanied by prompt response of the near-stream groundwater table in well N1, which is immediately adjacent to the stream (Figure 7). At well N1, the water table remained above the stream stage at all times, so the head gradient was in the streamward direction, and flow from the hillslope to the stream continued without interruption. The magnitude of the hydraulic gradient toward the stream declined across events, so the flow rate from the hillslope to the stream decreased at peak stream stage in each successive storm.

4.5. Transient Flow

[25] The groundwater model, calibrated for steady base flow conditions, was applied to the hydraulic data collected over the course of several small storm events. In general, the observed pressure heads at piezometers within the model domain were well modeled, except at the beginning and end of the events (Figure 8). For example, toward the end of event A, the model underpredicted the observed pressure head by ~0.05 m. The reason for this may be the model's failure to represent the impact of three-dimensional hydrologic processes on the riparian subsurface pressure field, but the generally good agreement between model and data argues that for the majority of the flood events, our assumption of a two-dimensional process is a reasonable simplification.

4.6. Transient Transport

[26] Temporal evolution of NO_3^- in stream water showed a "dilution" pattern during a 20-mm precipitation event on 27–30 October and 8–11 November 2006 (Figures 9 and 10). The groundwater flow and transport model, as calibrated to steady base flow conditions, was used to simulate the subsurface transport of NO_3^- during the storm. The results of the numerical simulation were in qualitative agreement with the observed NO_3^- evolution pattern. The

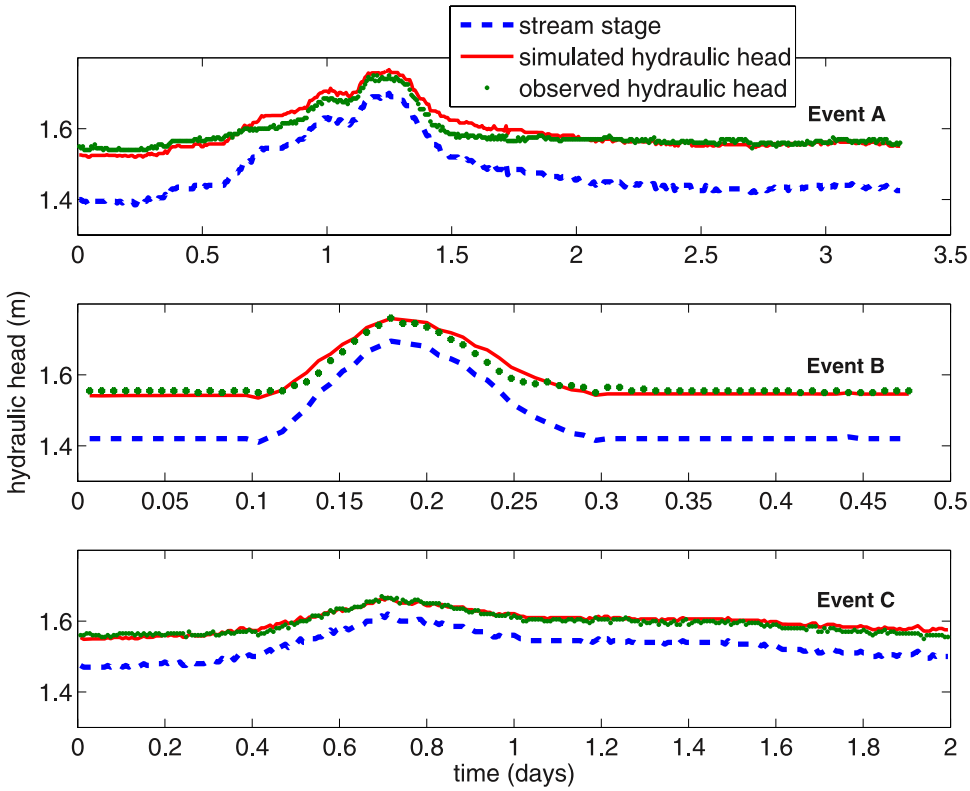

Figure 8. Comparison of observed hydraulic heads at well N1 during events A, B, and C to predictions from the two-dimensional finite element model. The dashed line is stream stage. The solid line denotes model prediction, and the dotted line denotes the field observations.

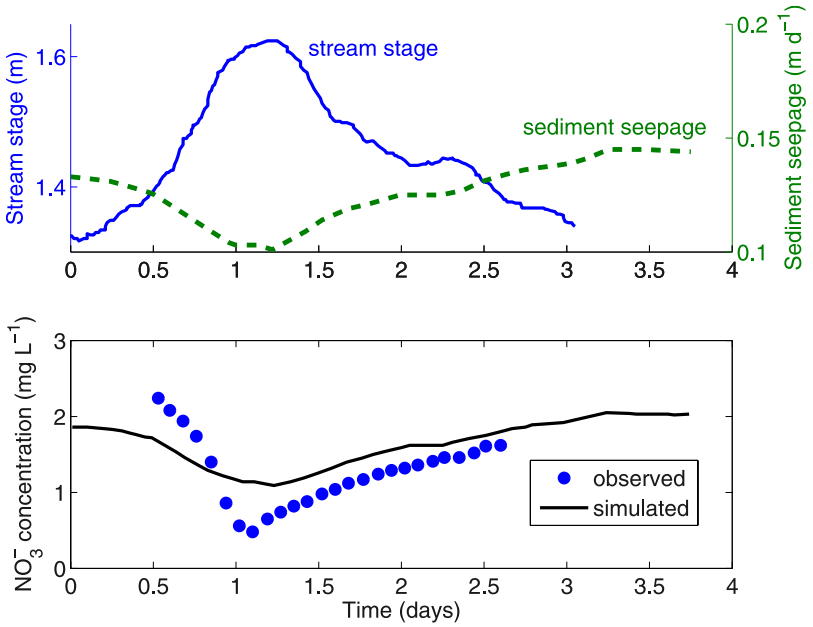

Figure 9. Temporal evolution of NO_3^- concentration, in mg NO_3^--N L^{-1}, in the stream during the storm event on 27–30 October 2006.

sediment seepage rate, the total water flux across the stream channel boundary, decreased on the rising limb of the hydrograph (Figure 9), reached a minimum at the stream stage peak, and then slowly increased through the hydrograph recession. After the flood wave passed, the seepage rate recovered to the preevent value. The mean residence time of water in the sediments can be estimated for flow conditions during the storm and for base flow conditions through particle tracking. A series of particles released along a vertical line 3 m from the stream and then traced to estimate residence times shows that residence times during the storm peak are about a factor of 2 larger than they are at base flow (Figure 11). The NO_3^- concentration deceased in response to the reduced seepage rate (longer residence time) that allowed greater denitrification [*Gu et al.*, 2007, 2008], reached a minimum slightly after the peak in stream stage, and then recovered in response to the increasing seepage rate (shorter residence time) (Figures 9 and 10).

5. Discussion

5.1. Transport of NO_3^- Under Steady Base Flow Conditions

[27] The flow paths through the hillslope control the transport of nitrate to the stream (Figure 4). Two main

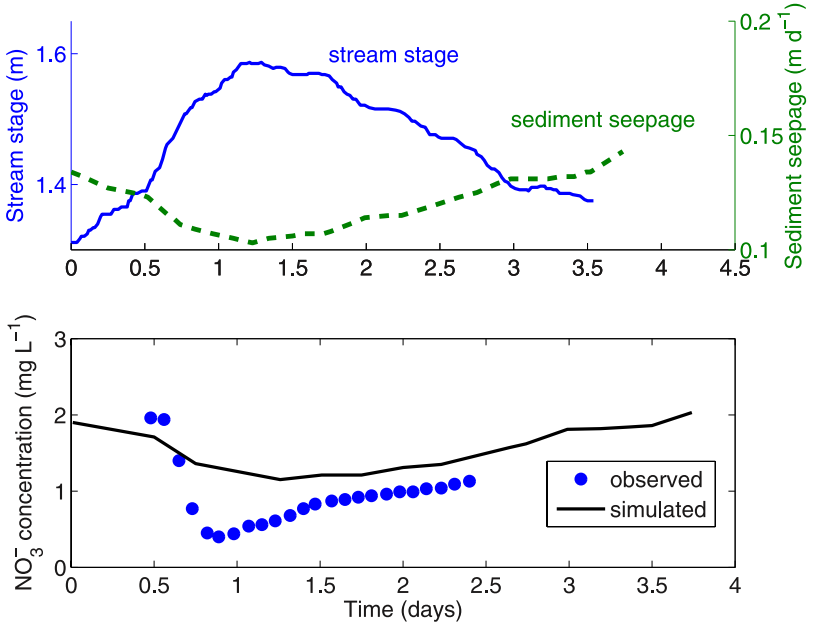

Figure 10. Temporal evolution of NO_3^- concentration, in mg NO_3^--N L^{-1}, in the stream during the storm event on 8–11 November 2006.

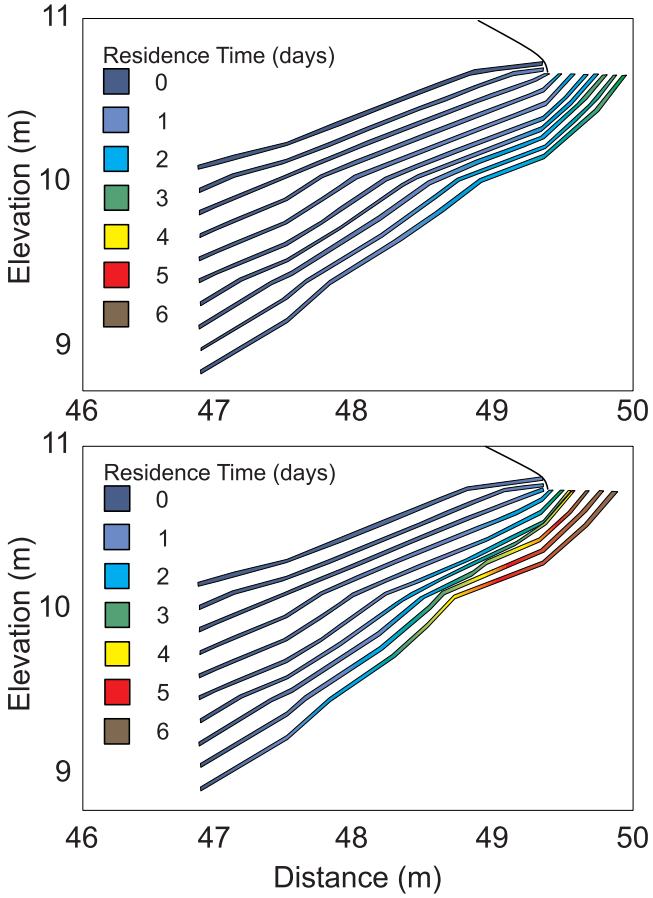

Figure 11. Particle residence times during (top) base flow and (bottom) storm illustrating the effect of stream-aquifer interaction.

water sources for the stream can be identified: an upward discharging, relatively deep path with a NO_3^- concentration >12 mg NO_3^--N L^{-1} and a relatively shallow (<2.5 m below ground surface) horizontal to subhorizontal path with a NO_3^- concentration of <6 mg NO_3^--N L^{-1}. The former presumably represents water originating from the fertilized field at the top of the slope, and the latter presumably represents water locally recharged in the near-stream riparian zone with a lower NO_3^- concentration. This interpretation is consistent with NO_3^- concentrations observed in shallow groundwater elsewhere [*Young and Briggs*, 2005].

[28] The model for nitrate flux from the groundwater to the stream was consistent with observed stream concentrations only when denitrification in streambed sediments was included. On the basis of the total discharge and NO_3^- reduction, we calculate a removal rate of NO_3^--N in the biogeochemically reactive zone around the channel of 3.39 g m^{-2} d^{-1}. This removal rate is about twice as much as the rate of 1.8 g m^{-2} d^{-1} reported for Smith Creek, Michigan [*Hedin et al.*, 1998], and 2 orders of magnitude greater than values in another riparian zone study [*Lowrance*, 1992]. We conclude that with a sufficient carbon source, the sediments near the groundwater-surface water interface possess a remarkable potential for NO_3^- removal from subsurface waters. In fact, according to our model results, removal rates were so rapid in our experimental transect that NO_3^- concentrations change from 12 mg NO_3^--N L^{-1} to as low as 0.1 mg NO_3^--N L^{-1} over as little as 30 cm of flow path.

5.2. Riparian Hydrology During Storms

[29] In locations where steeply sloping land borders a stream, the behavior of the water table within the riparian zone is largely determined by upslope conditions, and the influence of the adjacent river or stream on riparian soil hydrology will be limited. In a watershed where the riparian zone is flat, the water level in the river can have a strong influence on the riparian water table [*Burt et al.*, 2002]. At our experimental site, Cobb Mill Creek conforms to the former condition: a relatively steep slope directly borders the stream, and thus there will rarely be a hydraulic gradient away from the stream toward the land. The hydraulic gradient toward the stream is diminished during the passage of a flood wave (Figure 8), however, and flow rates through and residence times within the streambed sediments are affected. Unlike the extensive bank storage (with reversed flow) that occurs in floodplain areas [*Bates et al.*, 2000; *Squillace*, 1996], the response to floods may be limited in hillslope areas without floodplains or riparian wetlands because of a much steeper hydraulic gradient toward the stream. In the present study, the effect of passage of a flood wave is to retard the flow of hillslope water to the stream during periods of high stream stage. The residence time of groundwater within the streambed sediments is increased during these periods, a condition that favors the biogeochemical reduction process (denitrification) that lowers NO_3^- concentrations. Roughly a 30% decrease in seepage rates, the inverse of which is a surrogate indication of residence time, was seen for the two storms sampled (Figures 9 and 10).

5.3. Nitrate Transport During Storms

[30] From an ecosystem perspective, the lateral linkage between streams and riparian zones during floods enhances the capacity of the subsurface to retain the hillslope runoff and to limit the flux of chemical constituents to the stream. Retention of nonreactive solutes is temporary because they will be transported to the stream during and following the streamflow recession. Reactive solutes may experience losses, however (e.g., to the atmosphere via denitrification), and thus the total load delivered to the stream may be decreased.

[31] For systems that experience an extensive degree of bank storage (i.e., flow reversals so that significant quantities of stream water are stored temporarily in stream banks), it is clear that a major effect on nitrate fluxes can ensue [*Burt et al.*, 1999; *Marti et al.*, 2000]. For example, at Cedar River, Iowa, a 2-m rise in river stage caused bank storage water to move horizontally at least 30 m into an alluvial aquifer and vertically about 4 m below the river bottom [*Squillace*, 1996]. In the present study, we have shown that even in a stream with steep banks, the biogeochemical reactions in the sediments underlying the streambed influence not only base flow nitrate flux but also stormflow nitrate flux.

[32] The steep hillslopes combined with well-drained soil at our site expedited the movement of subsurface storm runoff carrying NO_3^-. The change in biologically reactive solute transport to the stream during floods will be controlled by hydrological residence time and rates and types

of biochemical processes near the groundwater-surface water interface [*Burt and Pinay*, 2005; *Triska et al.*, 1993]. For the two floods studied in 2006, concentrations of nitrate in stream water had a significant dip that is consistent with the "dilution effect" found in agricultural catchments under some conditions [*Poor and McDonnell*, 2007]. While these authors argued that the dilution was mainly caused by mixing with low-nitrate soil water, the present study suggests that in some situations biological processes can play an important role in nitrate concentration reduction. In other words, biotic removal can occur in addition to simple dilution. There are other instances, however, such as large storms or flat landscapes (i.e., floodplains), in which the increased flux on the flood recession can be dominant, leading to a net increase in NO_3^- loading [*Gu et al.*, 2008].

5.4. Summary

[33] One question that we posed at the start of this paper was whether our inferences, drawn from laboratory experiments, that nitrate reduction in streambed sediments explained the observed differences between groundwater NO_3^- concentrations and those in Cobb Mill Creek itself remained reasonable once multidimensional groundwater flow paths along with dilution from lower-nitrate riparian waters were taken into account. Our results indicate that this is indeed the case. That is, the steady state coupled flow and transport model used to interpret field data is consistent with observations only when high rates of denitrification in the streambed sediments are included.

[34] Another question that we posed related to the effect of temporal variation in stream stage on nitrate concentrations. Our contention was that transient hydrological events can play an important role in episodic NO_3^- loading during storms as a result of stream-groundwater interactions in streambed sediments. Our results indicate that changes in the residence time of groundwater upwelling through streambed sediments during storm events can indeed have a significant effect on the flux of nitrate to the stream.

[35] The overarching question we set out to address spoke to the adequacy of a reactive transport model driven by groundwater heads in describing nitrate flux to a stream under both base flow and storm event conditions. In point of fact, we were able to describe long-term base flow behavior as well as storm event nitrate fluxes from this small stream. The processes identified in this paper will generally apply to stream systems with steeply sloping banks and well-drained aquifer material. The interactions between subsurface stormflow and the spatial response patterns in the riparian zone are obviously site specific, controlled by local topography and hydrogeologic setting. Nevertheless, the geomorphology of this study site is typical of many coastal streams in the eastern United States; the processes identified herein should be common for this class of system.

Appendix A: Model Details

A1. Groundwater Flow Model

[36] The model describes time-dependent unconfined (i.e., with a free surface) saturated-unsaturated groundwater flow [*Bear*, 1972]. In notation used by *Neuman and Witherspoon* [1971], the model reads

$$\frac{\partial}{\partial x_i}\left(K_r K_i \frac{\partial h}{\partial x_i}\right) = (S_w S_s + C(\psi))\frac{\partial h}{\partial t} \tag{A1}$$

where x_i is the horizontal and vertical coordinate directions [L]; K_i is the principal components of the hydraulic conductivity tensor, aligned to be colinear with the x and z directions [L/T]; Kr is relative permeability, assumed to be a scalar function of water saturation [L/T]; S_w is water saturation, which varies between 0 for dry conditions and 1 for saturated conditions [dimensionless]; S_s is specific storage [1/L]; h is hydraulic head [L]; C is specific moisture capacity, equal to $\theta \frac{dS_w}{d\psi}$, where θ is porosity [dimensionless] and ψ is pressure head, equal to $h-z$, where z is elevation head [L], and t is time [T].

[37] Equation (A1) contains two parameters, K and C, for which functional relationships must be specified. Relationships between water saturation and pressure head and between water saturation and relative permeability are nonlinear. We used the relationships proposed by *Brutsaert* [1966] and also used by *Winter* [1983].

[38] Normalized water saturation can be specified as

$$S_{wD} = \frac{A}{(-\psi)^c + A} \tag{A2}$$

where

$$S_{wD} = \frac{S_w - S_{wr}}{1 - S_{wr}} \tag{A3}$$

S_{wr} is residual, or nonmoving water saturation, and A and c are empirical parameters.

[39] Relative permeability is specified as

$$K_r = S_{wD}^d \tag{A4}$$

where d is an empirical parameter.

[40] Parameters of the porous medium were prescribed on the basis of regional slug tests and laboratory falling head tests. These measurements indicated an average saturated hydraulic conductivity of 5×10^{-3} cm s^{-1} for the aquifer [*Hubbard et al.*, 2001] and a vertical saturated hydraulic conductivity of 4×10^{-4} cm s^{-1} for the stream channel materials [*Gu*, 2007]. Spatially uniform material properties were used and were represented by a Brooks and Corey soil water retention model [*Brooks and Corey*, 1966] with the residual and saturated moisture contents set at values for a sandy soil (Table 1).

A2. Solute Transport

[41] The differential equation describing mass transport and dispersion of dissolved constituents in a saturated or partially saturated porous medium can be written in two dimensions [*Bear*, 1972] as

$$\frac{\partial c}{\partial t} = \frac{\partial}{\partial x_i}\left(\theta D_{ii}\frac{\partial c}{\partial x_i} + \theta D_{ij}\frac{\partial c}{\partial x_j}\right) - q_i\frac{\partial c}{\partial x_i} - R \tag{A5}$$

in which c is concentration of solute, D_{ij} is the hydrodynamic dispersion tensor, q is specific discharge (Darcy velocity), θ is effective porosity, and R is a reaction term.

[42] Since it is impractical to evaluate all the components of the dispersion tensor, it is generally assumed that the porous medium is isotropic with respect to dispersion. Using this assumption, *Bear* [1972] expressed the hydrodynamic dispersion coefficient as

$$D_{xx} = \alpha_L v_x^2/v + \alpha_T v_y^2/v$$

$$D_{yy} = \alpha_L v_y^2/v + \alpha_T v_x^2/v \tag{A6}$$

$$D_{xy} = D_{yx} = (\alpha_L - \alpha_T) v_x v_y/v$$

where α_L is longitudinal dispersivity of the porous medium (in the direction of flow); α_T is transverse dispersivity of the porous medium (normal to the direction of flow); v_x, v_y are components of the seepage velocity in the x and y directions, respectively; and v is the magnitude of the velocity.

[43] We used a multiple-Monod equation to describe microbial reactions (R in the equation above). Biological reactions simulated included aerobic respiration of dissolved organic matter followed by denitrification. Noncompetitive inhibition was used to suppress denitrification while dissolved oxygen was present. Full details are given by *Gu et al.* [2007].

A3. Numerical Solution

[44] The Galerkin finite element method was used to determine approximate solutions to equations (A1) and (A5) under the appropriate initial and boundary conditions. For the hillslope problem, a triangular mesh with greater resolution near the stream was used (Figure 3). The mesh consists of 1652 elements and 886 nodes with element sizes varying from 0.2 m at the stream channel to 2.5 m at the upland and base of aquifer.

[45] As suggested by *Neuman* [1973], we defined the nodal values of the time derivatives as weighted averages over the entire flow region according to

$$\frac{\partial h}{\partial t} = \frac{\sum_e \int_{\Omega^e} (S_w S_s + C) \dfrac{\partial h}{\partial t} N_i dx dz}{\sum_e \int_{\Omega^e} (S_w S_s + C) N_i dx dz} \tag{A7}$$

where the N_i are linear basis functions.

[46] A functional representation of the parameters K and C [*Neuman*, 1973; *Pinder et al.*, 1973] within an element can be assumed to vary linearly using the same set of spatial functions N_i in the form

$$K = K_l(\psi) N_i, S_w = S_w(\psi) N_i, \text{ and } C = C_l(\psi) N_i \tag{A8}$$

The resulting set of finite element equations for water flow can be written in matrix form as

$$G\{h\} + H\left\{\frac{\partial h}{\partial t}\right\} + E = 0 \tag{A9}$$

where G and H are $n \times n$ matrices and E is a vector of length n. The time-dependent nature of equations (A1) and (A5) can be accommodated by employing a finite difference scheme to approximate the time derivatives. Employing a fully implicit backward difference scheme in terms of h in equation (A9) yields

$$\left(G_{ij}^k + \frac{1}{\Delta t^k} H_{ij}^k\right) h_I^{k+1} = \frac{1}{\Delta t^k} H_{ij}^k h_i^k - E_I^k \tag{A10}$$

where k indicates the time t^k and $\Delta t^k = t^{k+1} - t^k$. The Douglas-Jones predictor-corrector method for the solution of equation (A10) is described by the following: Predictor equation

$$\left(G_{ij}^k + \frac{1}{\Delta t^k/2} H_{ij}^k\right) h_i^{k+1/2} = \frac{1}{\Delta t^{k/2}} H_{ij}^k h_I^k - E_i^k \tag{A11}$$

Corrector equation

$$\left(G_{ij}^{k+1/2} + \frac{1}{\Delta t^k} H_{ij}^{k+1/2}\right) h_i^{k+1} = \frac{1}{\Delta t^k} H_{ij}^{k+1/2} h_i^k - E_i^{k+1/2} \tag{A12}$$

[47] **Acknowledgments.** This research was supported by funding from the National Science Foundation under NSF-EAR 0208386. The Virginia Coast Reserve LTER, funded by the National Science Foundation, provided accommodations and logistical support during the field work. We are indebted to Anna Sofranko for her enthusiastic assistance in the field.

References

Bates, P. D., M. D. Stewart, A. Desitter, M. G. Anderson, J. P. Renaud, and J. A. Smith (2000), Numerical simulation of floodplain hydrology, *Water Resour. Res.*, *36*(9), 2517–2529, doi:10.1029/2000WR900102.

Bear, J. (1972), *Dynamics of Fluids in Porous Media*, 764 pp., Elsevier, New York.

Böhlke, J. K., E. M. O'Connell, and K. L. Prestegaard (2007), Ground water stratification and delivery of nitrate to an incised stream under varying flow conditions, *J. Environ. Qual.*, *36*, 664–680, doi:10.2134/jeq2006.0084.

Brooks, R. H., and A. T. Corey (1966), Properties of porous media affecting fluid flow, *J. Irrig. Drain. Am. Soc. Civ. Eng.*, *92*, 61–88.

Brusseau, M. L., M. Q. Hu, J. M. Wang, and R. M. Maier (1999), Biodegradation during contaminant transport in porous media. 2. The influence of physicochemical factors, *Environ. Sci. Technol.*, *33*(1), 96–103, doi:10.1021/es980311y.

Brutsaert, W. (1966), Probability laws for pore-size distributions, *Soil Sci.*, *101*, 85–92, doi:10.1097/00010694-196602000-00002.

Burt, T. P., and G. Pinay (2005), Linking hydrology and biogeochemistry in complex landscapes, *Prog. Phys. Geogr.*, *29*(3), 297–316, doi:10.1191/0309133305pp450ra.

Burt, T. P., L. S. Matchett, K. W. T. Goulding, C. P. Webster, and N. E. Haycock (1999), Denitrification in riparian buffer zones: The role of floodplain hydrology, *Hydrol. Processes*, *13*(10), 1451–1463, doi:10.1002/(SICI)1099-1085(199907)13:10<1451::AID-HYP822>3.0.CO;2-W.

Burt, T. P., P. D. Bates, M. D. Stewart, A. J. Claxton, M. G. Anderson, and D. A. Price (2002), Water table fluctuations within the floodplain of the River Severn, England, *J. Hydrol.*, *262*(1–4), 1–20, doi:10.1016/S0022-1694(01)00567-4.

Sinnott, A., and G. C. Tibbits Jr. (1968), Ground-water resources of Accomack and Northampton counties, Virginia, *Rep. 9*, 113 p., Va. Div. of Miner. Resour., Richmond, Va.

Galavotti, H. (2004), Spatial profiles of sediment denitrification at the ground water-surface water interface in Cobb Mill Creek on the Eastern Shore of Virginia, M.S. thesis, Univ. of Va., Charlottesville.

Gu, C. (2007), Hydrological control on nitrate delivery through the groundwater surface water interface, Ph.D. thesis, 250 pp., Univ. of Va., Charlottesville.

Gu, C., G. M. Hornberger, A. L. Mills, J. S. Herman, and S. A. Flewelling (2007), Nitrate reduction in streambed sediments: Effects of flow and biogeochemical kinetics, *Water Resour. Res.*, *43*, W12413, doi:10.1029/2007WR006027.

Gu, C., G. M. Hornberger, J. S. Herman, and A. L. Mills (2008), Effect of freshets on the flux of groundwater nitrate through streambed sediments, *Water Resour. Res.*, *44*, W05415, doi:10.1029/2007WR006488.

Hedin, L. O., J. C. von Fischer, N. E. Ostrom, B. P. Kennedy, M. G. Brown, and G. P. Robertson (1998), Thermodynamic constraints on nitrogen transformations and other biogeochemical processes at soil-stream interfaces, *Ecology*, *79*(2), 684–703.

Hill, A. R. (1996), Nitrate removal in stream riparian zones, *J. Environ. Qual.*, *25*, 743–755.

Hill, A. R., K. J. Devito, S. Campagnolo, and K. Sanmugadas (2000), Subsurface denitrification in a forest riparian zone: Interactions between hydrology and supplies of nitrate and organic carbon, *Biogeochemistry*, *51*(2), 193–223, doi:10.1023/A:1006476514038.

Hornberger, G., and P. Wiberg (2005), *Numerical Methods in the Hydrological Sciences* [electronic], *Spec. Publ. Ser.*, vol. 57, 233 pp., AGU, Washington, D. C.

Hubbard, S. S., J. Chen, J. Peterson, E. L. Majer, K. H. Williams, D. J. Swift, B. Mailloux, and J. Rubin (2001), Hydrological characterization of the South Oyster bacterial transport site using geophysical data, *Water Resour. Res.*, *37*(10), 2431–2456, doi:10.1029/2001WR000279.

Inamdar, S. P., and M. J. Mitchell (2006), Hydrologic and topographic controls on storm-event exports of dissolved organic carbon (DOC) and nitrate across catchment scales, *Water Resour. Res.*, *42*, W03421, doi:10.1029/2005WR004212.

Lowrance, R. (1992), Groundwater nitrate and denitrification in a coastal plain riparian forest, *J. Environ. Qual.*, *21*, 401–405.

Marti, E., S. G. Fisher, J. D. Shade, and N. A. Grimm (2000), Flood frequency and stream-riparian linkages in arid lands, in *Streams and Groundwaters*, edited by J. B. Jones and P. J. Mulholland, pp. 111–136, Academic, San Diego, Calif.

Mills, A. L., G. M. Hornberger, and J. S. Herman (2008), Sediments in low-relief coastal streams as effective filters of agricultural nitrate, paper presented at Specialty Conference on Riparian Processes, Am. Water Resour. Assoc., Norfolk, Va.

Mixon, R. B. (1985), Stratigraphic and geomorphic framework of uppermost Cenozoic deposits in the southern Delmarva Peninsula, Virginia and Maryland, *U.S. Geol. Surv. Prof. Pap., 1067-C*.

Mixon, R. B., C. R. Berquist Jr., W. L. Newell, and G. H. Johnson (1989), Geologic map and generalized cross sections of the coastal plain and adjacent parts of the Piedmont, Virginia, *U.S. Geol. Surv. Misc. Invest. Ser.*, *I-2033*, 3 sheets.

Neuman, S. P. (1973), Saturated-unsaturated seepage by finite elements, *J. Hydraul. Div. Am. Soc. Civ. Eng.*, *99*(12), 2233–2250.

Neuman, S. P., and P. A. Witherspoon (1971), Analysis of nonsteady flow with a free surface using the finite element method, *Water Resour. Res.*, *7*(3), 611–623, doi:10.1029/WR007i003p00611.

Ocampo, C. J., C. E. Oldham, and M. Sivapalan (2006), Nitrate attenuation in agricultural catchments: Shifting balances between transport and reaction, *Water Resour. Res.*, *42*, W01408, doi:10.1029/2004WR003773.

Pinder, G. F., E. O. Frind, and S. S. Papadopolous (1973), Functional coefficients in analysis of groundwater flow, *Water Resour. Res.*, *9*(1), 222–226, doi:10.1029/WR009i001p00222.

Poor, C. J., and J. J. McDonnell (2007), The effects of land use on stream nitrate dynamics, *J. Hydrol.*, *332*(1–2), 54–68, doi:10.1016/j.jhydrol.2006.06.022.

Puckett, L. J., and W. B. Hughes (2005), Transport and fate of nitrate and pesticides: Hydrogeology and riparian zone processes, *J. Environ. Qual.*, *34*, 2278–2292, doi:10.2134/jeq2005.0109.

Sofranko, A. (2007), Nitrate flux during storm events on the Eastern Shore of Virginia, B.S. thesis, Univ. of Va., Charlottesville.

Squillace, P. J. (1996), Observed and simulated movement of bank-storage water, *Ground Water*, *34*, 121–134, doi:10.1111/j.1745-6584.1996.tb01872.x.

Triska, F. J., J. H. Duff, and R. J. Avanzino (1993), The role of water exchange between a stream channel and its hyporheic zone in nitrogen cycling at the terrestrial aquatic interface, *Hydrobiologia*, *251*(1–3), 167–184, doi:10.1007/BF00007177.

Winter, T. C. (1983), The interaction of lakes with variably saturated porous-media, *Water Resour. Res.*, *19*(5), 1203–1218, doi:10.1029/WR019i005p01203.

Young, E. O., and R. D. Briggs (2005), Shallow ground water nitrate-N and ammonium-N in cropland and riparian buffers, *Agric. Ecosyst. Environ.*, *109*(3–4), 297–309, doi:10.1016/j.agee.2005.02.026.

C. Gu, Berkeley Water Center, University of California, 413 O'Brien Hall, Berkeley, CA 4720-1718, USA. (cgu@berkeley.edu)

J. S. Herman and A. L. Mills, Department of Environmental Sciences, University of Virginia, Charlottesville, VA 22904-4123, USA. (jherman@virginia.edu; amills@virginia.edu)

G. M. Hornberger, Department of Civil and Environmental Engineering, Vanderbilt University, VU Station B 351831, 2301 Vanderbilt Place, Nashville, TN 37235-1831, USA. (gmh3k@cms.mail.virginia.edu)